

Geophysical Research Letters

RESEARCH LETTER

10.1029/2019GL082089

Key Points:

- The evolution of moist entropy through monsoon onset features two distinct stages: gradual accumulation and abrupt increase
- The onset of the South Asian summer monsoon is marked by a sudden increase in radiative heating and surface latent flux
- Without cloud-radiative and wind-evaporation feedbacks, the monsoon experiences much smoother onset

Correspondence to:

J. Nie,
jinie@pku.edu.cn

Citation:

Ma, D., Sobel, A. H., Kuang, Z., Singh, M. S., & Nie, J. (2019). A moist entropy budget view of the South Asian summer monsoon onset. *Geophysical Research Letters*, 46. <https://doi.org/10.1029/2019GL082089>

Received 30 JAN 2019

Accepted 3 APR 2019

Accepted article online 8 APR 2019

A Moist Entropy Budget View of the South Asian Summer Monsoon Onset

Ding Ma¹ , Adam H. Sobel² , Zhiming Kuang³ , Martin S. Singh⁴ , and Ji Nie⁵ 

¹The Earth Institute, Columbia University, New York, NY, USA, ²Department of Applied Physics and Applied Mathematics, Department of Earth and Environmental Sciences, and Lamont-Doherty Earth Observatory, Columbia University, New York, NY, USA, ³Department of Earth and Planetary Sciences and School of Engineering and Applied Sciences, Harvard University, Boston, MA, USA, ⁴School of Earth, Atmosphere and Environment, Monash University, Melbourne, Victoria, Australia, ⁵Department of Atmospheric and Oceanic Sciences, Peking University, Beijing, China

Abstract Using a high-resolution global model with explicit representation of convection, the physical processes involved in the abrupt onset of South Asian summer monsoon are investigated within a moist entropy budget framework. The monsoon onset is a two-stage transition. During the first stage, which starts around 2 months before onset, the source terms of column-integrated moist entropy gradually increase, while the export by the large-scale circulation slowly strengthens. The second stage is marked by a sudden increase of radiative heating and surface latent heat flux 10 days prior to the onset, followed by abrupt strengthening of large-scale export of moist entropy. When either cloud-radiative or wind-evaporation feedback is disabled in numerical experiments, the monsoon experiences much smoother and weaker onset. The evolution of the system in a gross moist stability plane demonstrates that these positive feedbacks destabilize the system and are responsible for the abruptness of the transition.

1. Introduction

The start of the monsoon is characterized by an abrupt dry-wet transition, known as monsoon onset. The timing of monsoon onset has critical societal impact; a delayed monsoon onset is usually associated with drought and heat waves, while an early monsoon onset often leads to regional floods (Collier & Webb, 2002; Webster et al., 1998). Most global climate models (GCMs) are still unable to capture the onset of observed monsoon precipitation (e.g., Dong et al., 2014; Sperber et al., 2014; Wang et al., 2004). The inability of current models to accurately represent the timing, spatial distribution, and magnitude of monsoon precipitation also raises the concern that projections of future changes of the monsoon based on simulations with these models may be unreliable.

Improved theoretical understanding of the mechanisms of the monsoon and its onset is desirable to guide our understanding of model biases and provide a path to improving future projections under climate change. The classic theory holds that the angular momentum conserving global Hadley circulation, of which the monsoon is a regional expression, is fundamentally nonlinear, and a critical condition for the development of an axisymmetric meridional circulation is responsible for the abrupt monsoon onset (Held & Hou, 1980; Lindzen & Hou, 1988; Plumb & Hou, 1992). New dynamical arguments have been proposed in recent years, emphasizing the roles of eddies and advection of momentum, moisture, or moist static energy (e.g., Bordoni & Schneider, 2008; Prive & Plumb, 2007; Shaw, 2014; Schneider et al., 2014; Schneider & Bordoni, 2008; Xie & Saiki, 1999). Most of these studies rely on simulations with idealized topography and simple parameterizations of convection and radiation. Here we will focus on the realistic South Asian monsoon with more complex topography and representations of physical processes in the model.

A more recent interpretation of the South Asian monsoon system emphasizes the convectively coupled dynamics, as the interaction between convection and large-scale circulation lies at the heart of the system (see review by Boos, 2015). The theory of convective quasi-equilibrium assumes that moist convection is a fast process that maintains a state of quasi-equilibrium between convection and large-scale forcing in the tropical atmosphere, so that temperature nearly follows a moist adiabatic lapse rate in the troposphere above cloud base (Emanuel et al., 1994). As a result, the strength of the monsoon circulation is related to the meridional distribution of boundary layer moist entropy, and the thermal forcing for the monsoon may be interpreted in the context of processes contributing to the horizontal moist entropy gradient

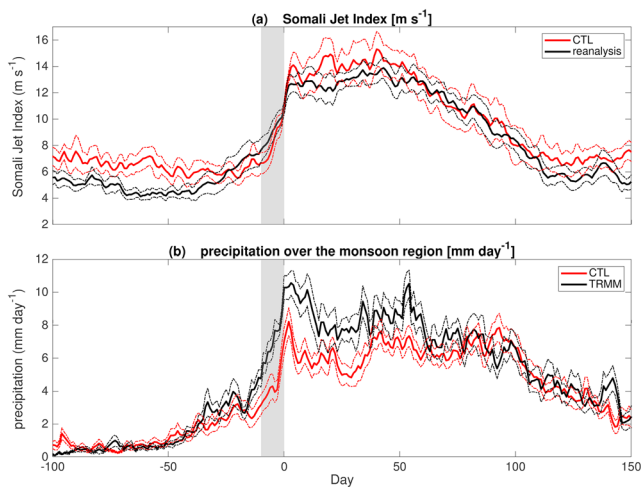


Figure 1. Composite evolution of (a) the Somali jet index and (b) averaged precipitation over the South Asian monsoon region in the control simulation (red) and reanalysis data or satellite observation (black). The dashed curves denote 95% confidence intervals. The day of onset is shifted to Day 0. The gray shading marks the period from Day -10 to Day 0. CTL = control run; TRMM = Tropical Rainfall Measuring Mission.

(Boos & Kuang, 2010; Emanuel, 1995; Nie et al., 2010; Singh et al., 2017). Within the framework of convective quasi-equilibrium, Boos and Emanuel (2009) found concurrent evolution of the surface enthalpy flux, the boundary layer moist entropy distribution, and the strength of the monsoon circulation, which supports the hypothesis that wind-evaporation feedback plays an important role in the abrupt onset of the South Asian monsoon. In addition, it has been shown that enhanced convection-wind-evaporation feedback is associated with an unrealistically strong Asian monsoon in a superparameterization GCM (Luo & Stephens, 2006), and the East Asian monsoon becomes weaker when the cloud-radiative feedback is disabled (Guo et al., 2015). These numerical studies focus on the monsoon strength in the mature stage, and yet it remains unclear how these processes influence the dry-wet transition, which is the emphasis of the present study.

We propose to understand the South Asian monsoon onset by diagnosing the column-integrated moist entropy budget in numerical simulations. In particular, we attempt to address the following questions. How does the moist entropy, and its sources and sinks, evolve during the transition? What are the key processes responsible for the abrupt onset? This approach is motivated by recent studies, which have used similar diagnostics to understand the Madden-Julian oscillation (MJO; e.g., Andersen & Kuang, 2012; Maloney, 2009; Sobel et al., 2014). The MJO has been hypothesized to be a moisture mode, so that the growth and propagation

of the MJO are considered to be consequences of processes (e.g., radiative heating and surface heat fluxes) contributing to the column-integrated moist static energy budget (e.g., Fuchs & Raymond, 2002; Sobel & Maloney, 2012). The South Asian monsoon is similar to the MJO in the sense that convectively coupled dynamics play an essential role in the system.

The next section introduces the numerical experiments and data used in this study, followed by the results from the simulations. We conclude with a short summary and brief discussions.

2. Numerical Experiments and Data

Four sets of global simulations were conducted using WRF Version 3. All integrations were performed with a horizontal grid spacing of 40 km and 40 vertical levels with prescribed sea surface temperature from the National Centre for Environmental Prediction final analysis data (National Centers for Environmental Prediction/National Weather Service/NOAA/U.S. Department of Commerce, 2000). Convection is explicitly simulated following the method of reduced acceleration in the vertical (Kuang et al., 2005), which rescales convective motions and large-scale circulations and allows global integrations at coarser resolutions with explicit (rather than parameterized) convection. The details of the model configurations are the same as those in Ma et al. (2014). The control run (CTL) is integrated from 1 October 1998 to 31 December 2016, and the output data from the first 3 months are discarded.

The monsoon onset is defined based on the Somali jet index (SJI) following Boos and Emanuel (2009). The SJI is calculated as the square root of the spatial mean kinetic energy of horizontal winds at 850 hPa over 5°S to 20°N ; 50°E to 70°E using daily reanalysis data, and the monsoon onset date for each year is defined as the start of the first 3-day period, during which the SJI maintained a value more than one standard deviation above the 18-year mean. The average onset date is 9 June for the 18-year control run, 5 days later (not statistically significant at 95% confidence level) than that in the reanalysis data. As will be shown in the following section, two positive feedbacks, the cloud-radiative feedback and the wind-evaporation feedback, are found to play key roles in the abrupt onset of the monsoon. To test the sensitivity of the monsoon onset to these feedbacks, three additional sets of experiments with perturbed model physics are restarted 30 days before monsoon onset each year, and integrated until 30 September. In the experiment NoRAD, the cloud-radiative feedback is disabled using the Clouds On/Off Climate Interaction Experiment protocol (Stevens et al., 2012), which has been widely adopted (e.g., Crueger & Stevens, 2015; Fermepin & Bony, 2014). To be specific, clouds are made transparent to radiation over the South Asian monsoon region ($10^{\circ}\text{--}25^{\circ}\text{N}$;

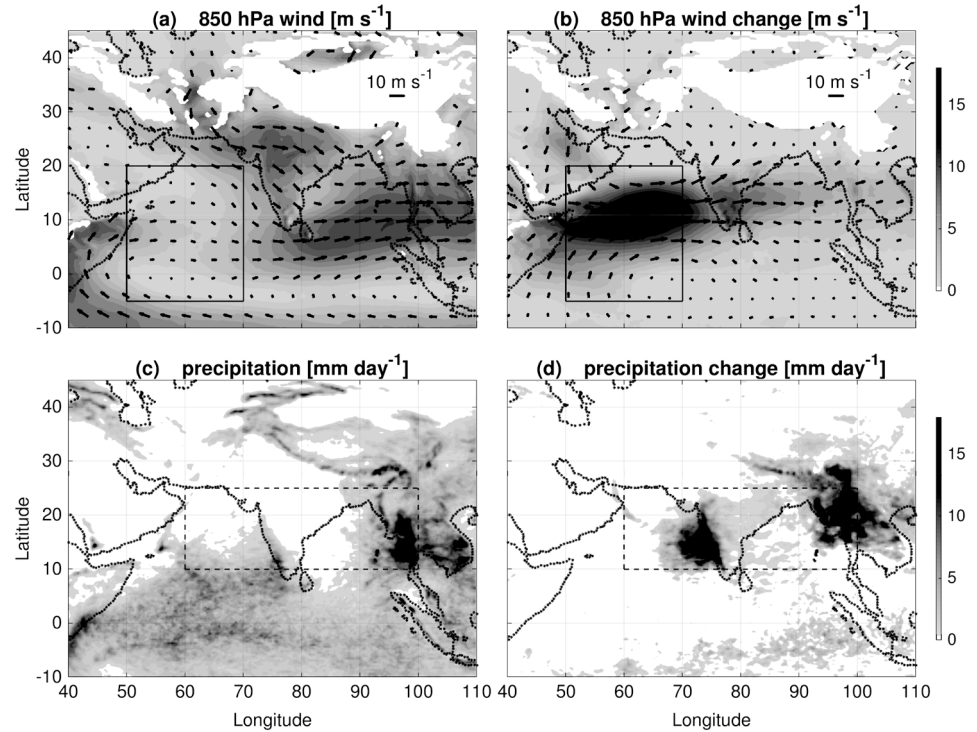


Figure 2. Composite of (a) 850-hPa winds and (c) precipitation 10 days before monsoon onset and composite change in (b) 850-hPa winds and (d) precipitation between Day -10 and Day 0 . The black box (a and b) denotes the region where the Somali jet index is computed, and the dashed box (c and d) denotes the region over which the precipitation and moist entropy budget is averaged.

60–100°E). The present method, rather than the commonly used way in which radiative heating is homogenized in space or time and the mean value is preserved (e.g., Andersen & Kuang, 2012), is chosen given the spatially inhomogeneous and temporarily transient nature of the monsoon onset. Also, Clouds On/Off Climate Interaction Experiment is able to test our hypothesis on the importance of cloud-radiative feedback at minimum cost, compared to the cloud-locking technique (e.g., Radel et al., 2009; Voigt & Shaw, 2015), which is computationally unaffordable with our high-resolution realistic simulations. Note that the radiative feedback from water vapor and temperature remains active in our NoRAD simulations, as the present study focuses on the cloud-radiative feedback. In the experiment NoFLX, the wind-evaporation feedback is turned off by prescribing the winds to the particular year's pre-monsoon-onset values in the surface flux parameterization when the latent and sensible heat fluxes are calculated over the South Asian monsoon region (10–25°N; 60–100°E). In the experiment NoPFB (i.e., No Positive Feedbacks), both of the cloud-radiative and wind-evaporation feedbacks are disabled.

The following column-integrated moist entropy budget equation is diagnosed:

$$\frac{\partial \langle h \rangle}{\partial t} = -\nabla \cdot \langle h \mathbf{v} \rangle + E + H + \langle R \rangle, \quad (1)$$

where the angle brackets denote mass-weighted column integration; h denotes the moist entropy and is approximated as $h = c_p \ln(\theta_e)$, in which c_p is the dry air heat capacity and θ_e is the equivalent potential temperature; \mathbf{v} is the horizontal velocity; and E , H , and R correspond to the contributions from surface latent heat flux, surface sensible heat flux, and radiative heating, respectively. Note that the entropy production by irreversible processes, such as molecular diffusion and evaporation of water condensate in unsaturated air, is neglected here, as the irreversible terms are a couple of orders of magnitude smaller than those we retain (Pauluis & Held, 2002a, 2002b; Singh & O'Gorman, 2016). Since h is approximately conserved in moist adiabatic processes, the latent heat release, which merely moves energy from the moisture component to the temperature component, is not a source term of h . Thus, the moist entropy equation has the advantage that the term associated with latent heat release, which is much larger than the surface fluxes and radiative heating in the dry static energy or dry entropy equation in the monsoon region, does not appear. In our

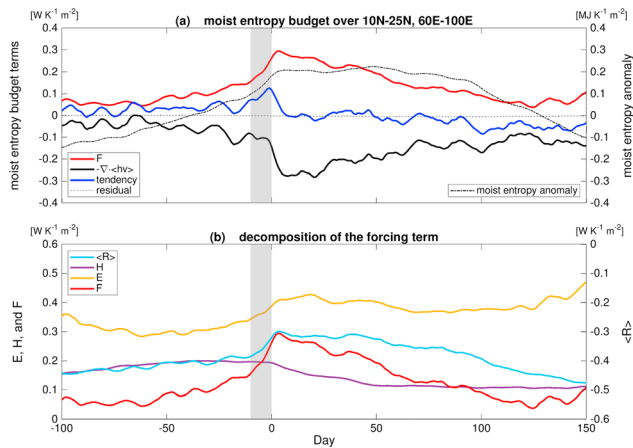


Figure 3. Composite evolution of column-integrated moist entropy budget averaged over 10–25°N; 60°E to 100°E in the control run. (a) The red, black, blue, and dashed curves denote the source term, the export by large-scale advection, the temporal tendency term, and the residual of the moist budget, respectively, and correspond to the left y axis. The dash-dotted curve denotes anomalous column-integrated moist entropy and corresponds to the right y axis. (b) The light blue curve denotes the contribution from radiative heating and corresponds to the right y axis. The purple, yellow, and red curves denote the sensible heat flux, the latent heat flux, and the sum of the source terms, respectively, and correspond to the left y axis.

ite change over the 10 days preceding the monsoon onset. Both compare well with those from the reanalysis data and observations (Boos & Emanuel, 2009). Before the onset of the Somali jet, the westerlies over the Arabian Sea in the Northern Hemisphere are weak, and the cross-equatorial flow is limited to a region west of 50°E (Figure 2a). The precipitation is weak in the Northern Hemisphere except for the west coast of Myanmar (Figure 2c). Over the 10 days preceding the onset, the westerlies are greatly enhanced over the northern Indian Ocean, leading to a strengthened the Somali jet (Figure 2b), and the precipitation in the monsoon region also increases significantly (Figure 2d).

The abrupt onset of the South Asian summer monsoon is interpreted using the column-integrated moist entropy budget, and the time series of the column-integrated moist entropy and its budget terms in equation (1) averaged over the South Asian monsoon region are shown in Figure 3a. The result indicates that the onset of the monsoon is a two-stage transition. The first stage, from around 2 months before monsoon onset to Day -10, features a gradual accumulation of moist entropy. The source term of $\langle h \rangle$ (i.e., $F = E + H + \langle R \rangle$; red curve in Figure 3a) also gradually increases, associated with the northward shift of solar insolation. The large-scale circulation exports moist entropy from the monsoon region to the surrounding regions (black curve in Figure 3a). The sum of the source terms and the large-scale export (i.e., the tendency of $\langle h \rangle$; blue curve in Figure 3a) is slightly positive. The second stage (from Day -10 to Day 0) corresponds to the monsoon onset, characterized by a sharp increase of $\langle h \rangle$, accompanied by a rapid increase in the moist entropy source term. Meanwhile, the export of moist entropy by large-scale circulation is only slightly enhanced. Since the migration of the maximum in solar insolation is a gradual process, the abrupt increase of moist entropy sources suggests positive feedbacks. At the end of the second stage, $\langle h \rangle$ approximately reaches its peak value, and the large-scale export jumps to the value that approximately balances the source terms. Following the monsoon onset is the mature stage of monsoon (Day 0 to around Day 100). During this period, the decrease in the strength of the source term and the large-scale export are synchronous and canceling each other, leaving $\langle h \rangle$ maintained at a nearly steady high value.

Figure 3b shows the three components of the moist entropy source, namely, the sensible heat flux (H), the latent heat flux (E), and the radiative heating ($\langle R \rangle$). During the first stage, all the three terms increase gradually, while E and $\langle R \rangle$ increase rapidly during monsoon onset. The concurrent rapid increases in the radiative heating, latent heat flux, and the strength of the monsoon suggest the potential roles of cloud-radiative and

diagnoses, all terms in equation (1) are integrated online at each time step during the simulations, rather than being calculated from snapshots of model output with comparatively coarse temporal resolution. As a consequence, we are able to close the moist entropy budget very well.

For model validation, the results of the control simulations are compared with ERA-Interim reanalysis (Dee et al., 2009) and Tropical Rainfall Measuring Mission (TRMM; Huffman et al., 2007) 3B42 daily precipitation.

3. Results

Following Boos and Emanuel (2009), a composite of the transition from a winter to a summer state is constructed based on the SJI. Figure 1a shows the resulting composite evolution of the SJI. In both the reanalysis data and control simulation, the strength of the Somali jet starts to increase abruptly 10 days prior to the onset and remains above 10 m/s for around 3 months after onset. The modeled SJI is overall around 1–2 m/s higher than that in the reanalysis data, but the control simulation is able to capture the abrupt onset of the SJI. Also, the present model well captures the abrupt increase of the precipitation in the monsoon region as in TRMM observations (Figure 1b), despite that the precipitation in the control run is around 2 mm/day weaker compared to TRMM precipitation from 10 days preceding monsoon onset to 50 days after onset.

The control simulations also reproduce realistic changes in the large-scale circulations and the spatial distribution of precipitation during monsoon onset. Figure 2 shows the modeled precipitation and 850-hPa horizontal winds 10 days before monsoon onset and the compos-

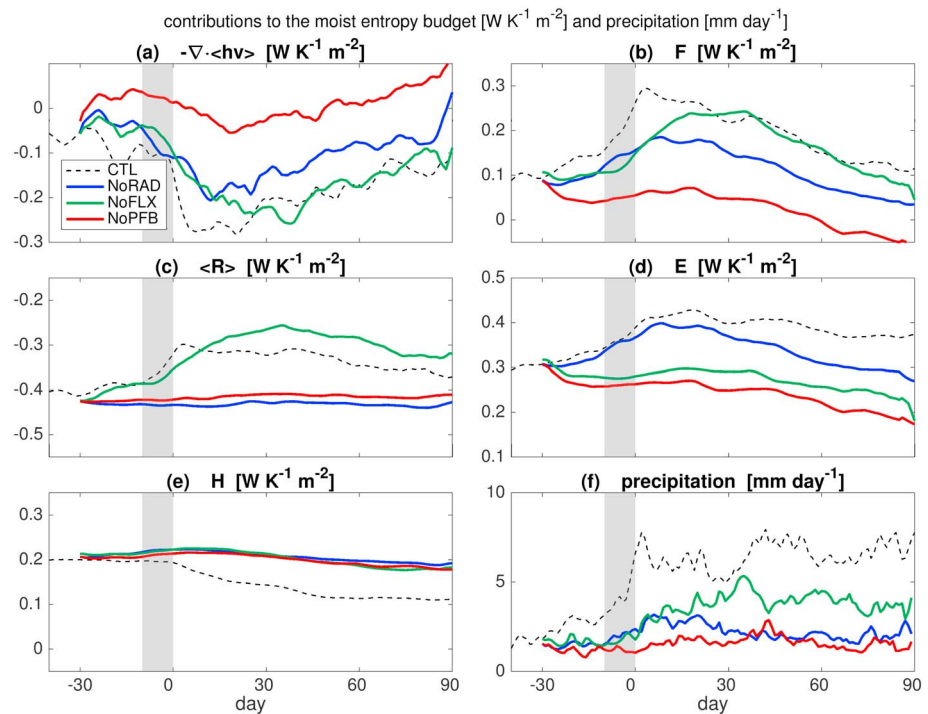


Figure 4. Composite evolution of column-integrated moist entropy budget terms (a–e) and precipitation (f) averaged over 10–25°N; 60°N to 100°E in the numerical simulations. The dashed, blue, green, and red curves denote the CTL, NoRAD, NoFLX, and NoPFB, respectively.

wind-evaporation feedbacks in the abrupt monsoon onset. After onset, E and R are nearly steady, while H decreases. Interestingly, the sensible heat flux decreases after monsoon onset, which is consistent with the decrease of surface temperature in the South Asian region (Boos & Emanuel, 2009; Hurley & Boos, 2013; Webster, 2004).

Numerical experiments are conducted to test the importance of these positive feedbacks. When the cloud-radiative feedback is turned off, the radiative heating decreases significantly (Figure 4c), mainly due to the absence of longwave heating by deep convective clouds. When the wind-evaporation feedback is disabled, the surface latent heat flux decreases significantly (Figure 4d). In the surface sensible heat flux (Figure 4e), the two perturbed experiments show slight increases, because the monsoon is much weaker so that the surface temperature is higher than in the control case. Nevertheless, in the perturbed experiments, the moist entropy source terms (Figure 4b) are significantly smaller than those in the control case. As a consequence, the large-scale circulation exports much less moist entropy in the experiments NoRAD and NoFLX than in the control (Figure 4a). When both of the positive feedbacks are disabled, the export of moist entropy by the large-scale circulation is even smaller, indicating almost full suppression of the large-scale circulation. The results from the numerical experiments can be summarized by the composite evolution of precipitation in the numerical experiments (Figure 4f). The monsoon region experiences much smoother increases in precipitation without these positive feedbacks. When the wind-evaporation feedback is turned off, the precipitation reaches its peak value 30 days later compared to the control, and the maximum precipitation rate is reduced by more than 2 mm/day. Bordoni and Schneider (2008) found the wind-evaporation feedback unnecessary for the monsoon onset in an aquaplanet GCM with a slab ocean, and the seeming conflict between their results and the present study might be attributed to the following two factors. First, the aquaplanet monsoon climatology is different from the present simulations, while homogeneities in topography may be associated with weaker monsoon winds and thus less important wind-evaporation feedback. Second, prescribed sea surface temperature, rather than an interactive slab ocean, could lead to a too strong wind-evaporation feedback. When the cloud-radiative feedback is disabled, the peak monsoon precipitation rate is reduced by more than 4 mm/day. The precipitation and the large-scale circulation show weak variations over the monsoon season when both of the positive feedbacks are disabled, indicating the failure of monsoon onset. These numerical experiments confirm that the positive feedbacks play essential roles in the

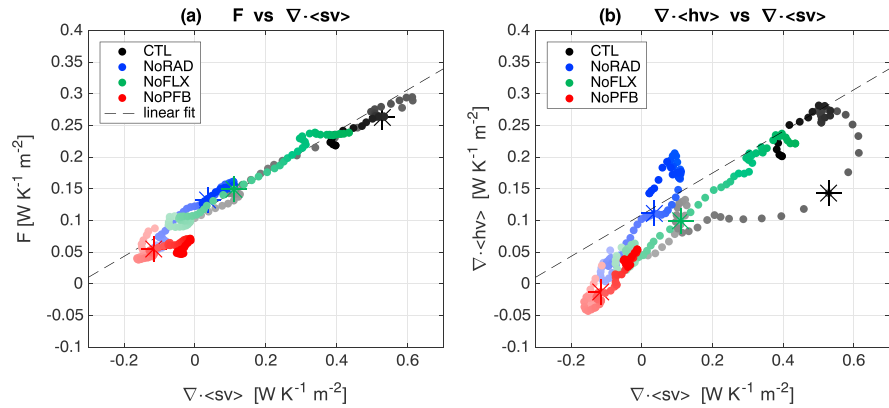


Figure 5. (a) Scatterplots of the sum of the source terms of column-integrated moist entropy against the divergence of column-integrated dry entropy. Each marker corresponds to 1 day from Day –30 to Day 30 with respect to the date of monsoon onset in CTL (denoted by the stars), and lighter colors indicate earlier dates. (b) The same as (a) but for the divergence of column-integrated moist entropy against the divergence of column-integrated dry entropy.

abrupt onset of the South Asian summer monsoon. In fact, without the positive feedbacks, the precipitation over the entire monsoon season weakens significantly. Luo and Stephens (2006) and Guo et al. (2015) have also shown the importance of the aforementioned feedbacks to the monsoon strength in the mature phase. Here we demonstrate and emphasize their essential roles during monsoon onset.

Last, we adopt the gross moist stability (GMS) plane (Inoue & Back, 2015, 2017), which has been used in diagnoses of convection and the MJO, to visualize the interaction between convection and large-scale circulations during monsoon onset. Dividing both sides of equation (1) by the divergence of column-integrated dry entropy ($s = c_p \ln \theta$, where θ is potential temperature), we may write

$$\nabla \cdot \langle s \mathbf{v} \rangle^{-1} \frac{\partial \langle h \rangle}{\partial t} = -(\Gamma - \Gamma_c), \quad (2)$$

in which

$$\Gamma = \frac{\nabla \cdot \langle h \mathbf{v} \rangle}{\nabla \cdot \langle s \mathbf{v} \rangle}, \quad (3)$$

and

$$\Gamma_c = \frac{F}{\nabla \cdot \langle s \mathbf{v} \rangle} = \frac{E + H + \langle R \rangle}{\nabla \cdot \langle s \mathbf{v} \rangle}. \quad (4)$$

Γ is the normalized GMS, representing how effectively the large-scale circulation can export moist entropy (Raymond et al., 2009). Γ_c measures the contribution of the diabatic source terms. Inoue and Back (2017) showed in observations that F is approximately linearly related to $\nabla \cdot \langle s \mathbf{v} \rangle$, which also holds for the monsoon simulations except the NoPFB case, in which the monsoon onset fails to occur. From Day –30 to Day 30 in CTL, NoRAD, and NoFLX, the diabatic source term and moist entropy divergence roughly lie on a straight line (Figure 5a). According to equation (2), if $\Gamma < \Gamma_c$, the moist entropy increases, indicating instability and growth of the monsoon. On the other hand, if $\Gamma > \Gamma_c$, the situation is stable, and the monsoon decays. Note that this relationship does not hold when convection is inactive (i.e., $\nabla \cdot \langle s \mathbf{v} \rangle$ is negative), and the discussion below only applies to the period when $\nabla \cdot \langle s \mathbf{v} \rangle$ is positive. On the GMS plane (Figure 5b), points below the critical line (dashed) correspond to $\Gamma < \Gamma_c$, indicating instability. The farther the data point from the line, the larger the moist entropy tendency is. Let us first examine CTL. Starting from Day –30, the monsoon system lies below the critical line and the monsoon is in its amplifying stage, consistent with the gradual increases of moist entropy and precipitation (Figures 1 and 3). Between Day –10 and Day 0, $\nabla \cdot \langle h \mathbf{v} \rangle$ remains more or less invariant as $\nabla \cdot \langle s \mathbf{v} \rangle$ rapidly increases, which indicates increases of moist entropy sources, due to the cloud-radiative and wind-evaporation feedbacks. The difference between Γ_c and Γ peaks at the time of onset, when the monsoon system is in its most unstable stage. After monsoon onset, the large-scale circulation develops in such a way that $\nabla \cdot \langle h \mathbf{v} \rangle$ catches up quickly and drives the system back to equilibrium. Correspondingly, in the GMS plane, the system moves toward the critical line and remains

close to the critical line after around 1 week. In contrast, the system remains close to the critical line in the experiments without cloud-radiative or wind-evaporation feedbacks. These results indicate that these positive feedbacks destabilize the system and facilitate an abrupt monsoon onset.

4. Summary

The start of the South Asian summer monsoon is characterized by a sudden dry-wet transition, known as monsoon onset, which is associated with a rapid reversal of the large-scale circulation interacting with monsoon convection. To explore the physical processes involved in the abrupt onset of South Asian summer monsoon, this study analyzes the column-integrated moist entropy budget over the South Asian monsoon region using high-resolution GCM simulations with an explicit representation of convection. The modeled monsoon compares well with reanalysis data and TRMM precipitation, although the average onset date is 9 June for the 18-year control run, 5 days later than that in the reanalysis.

The moist entropy budget indicates that the onset of the monsoon is a two-stage transition. During the first stage, which starts from around 2 months before onset, the export of column-integrated moist entropy by the large-scale circulation slowly increases, while the source of column-integrated moist entropy (i.e., the sum of surface fluxes and radiative heating) also gradually increases while the solar insolation shifts northward. The second stage (from Day -10 to Day 0) corresponds to the short period during which the monsoon transitions from a winter to a summer state, and it is marked by a sudden increase in the export of column-integrated moist entropy by the large-scale circulation, accompanied by rapid changes in the source terms in the moist entropy budget. The sudden increases in the moist entropy source terms suggest the importance of cloud-radiative and wind-evaporation feedbacks to the abrupt monsoon onset. When cloud-radiative and/or wind-evaporation feedbacks are disabled in numerical experiments, the corresponding source terms of moist entropy are significantly reduced, and the monsoon region experiences much smoother increases in precipitation, and the precipitation reaches substantially smaller values in the area and time mean over the entire monsoon. The evolution of the system in a GMS plane demonstrates the roles of the key components: The positive feedbacks destabilize the system and are responsible for the abruptness of the dry-wet shift.

The present results clearly show that the cloud-radiative and wind-evaporation feedbacks play important roles in the abrupt onset of South Asian summer monsoon. These positive feedbacks destabilize the monsoon system, and moist entropy source terms influence not just the onset but also the steady state value of the area-integrated precipitation in the monsoon region. One next step is to examine the prediction/predictability of the monsoon onset in GCMs, with foci on the physical processes associated with the positive feedbacks and the moisture field. Model biases in radiative heating, surface fluxes, and moisture will be analyzed aiming at model improvement. Another obvious next step is to investigate the physical processes associated with the retreat of the monsoon, which is a topic of considerable significance but attracts much less attention compared to monsoon onset.

This study examines the monsoon onset from a moist entropy budget view, and the dynamic aspect of monsoon is treated or diagnosed implicitly. The constraint of angular momentum of the large-scale circulation also plays important role during monsoon onset, and future work will combine the dynamic and thermodynamic consideration to provide a complete framework of monsoon onset as pointed out by Biasutti et al. (2018).

References

- Andersen, J. A., & Kuang, Z. (2012). Moist static energy budget of MJO-like disturbances in the atmosphere of a zonally symmetric aquaplanet. *Journal of Climate*, *25*(8), 2782–2804.
- Biasutti, M., Voigt, A., Boos, W. R., Braconnot, P., Hargreaves, J. C., Harrison, S. P., et al. (2018). Global energetics and local physics as drivers of past, present and future monsoons. *Nature Geoscience*, *11*, 392–400.
- Boos, W. R. (2015). A review of recent progress on Tibet's role in the South Asian monsoon. *CLIVAR Exchanges Special Issue on Monsoons*, *66*, 23–27.
- Boos, W., & Emanuel, K. (2009). Annual intensification of the Somali jet in a quasi-equilibrium framework: Observational composites. *Quarterly Journal of the Royal Meteorological Society*, *135*, 319–335.
- Boos, W. R., & Kuang, Z. (2010). Dominant control of the South Asian monsoon by orographic insulation versus plateau heating. *Nature*, *463*, 218–222.
- Bordoni, S., & Schneider, T. (2008). Monsoons as eddy-mediated regime transitions of the tropical overturning circulation. *Nature Geoscience*, *1*, 515–519.

Acknowledgments

The authors thank two anonymous reviewers for their helpful reviews. This work is supported by ONR grant GG010861 and NSF grant AGS-1759255. J. N. acknowledges supports from the National Natural Science Foundation of China grant 41875050. D. M. is supported by the Earth Institute Postdoctoral Fellowship. ERA-Interim reanalysis and TRMM precipitation data can be accessed at <https://apps.ecmwf.int/datasets/> and <https://pmm.nasa.gov/data-access/downloads/trmm>, respectively. The computations in this paper were run on the Odyssey cluster at Harvard University. Primary data and scripts used in the analysis are archived by the Research Computing Group at Harvard University and can be obtained by contacting the Harvard website (ithelp@harvard.edu).

- Collier, M., & Webb, R. (2002). *Floods, droughts, and climate change* (Vol. 66). Tucson: University of Arizona Press.
- Crueger, T., & Stevens, B. (2015). The effect of atmospheric radiative heating by clouds on the Madden-Julian Oscillation. *Journal of Advances in Modeling Earth Systems*, 7, 854–864. <https://doi.org/10.1002/2015MS000434>
- Dee, W., Uppala, S. M., Simmons, A. J., Berrisford, P., Poli, P., Kobayashi, S., et al. (2009). The ERA-Interim reanalysis: Configuration and performance of the data assimilation system. *Quarterly Journal of the Royal Meteorological Society*, 137, 553–597. <https://doi.org/10.1002/qj.828>
- Dong, G., Zhang, H., Moise, A., Hanson, L., Liang, P., & Ye, H. (2014). CMIP5 model-simulated onset, duration and intensity of the Asian summer monsoon in current and future climate. *Climate Dynamics*, 46, 355–382.
- Emanuel, K. (1995). On thermally direct circulations in moist atmospheres. *Journal of the Atmospheric Sciences*, 52, 1529–1534.
- Emanuel, K., Neelin, D., & Bretherton, C. (1994). On large-scale circulation in convecting atmospheres. *Quarterly Journal of the Royal Meteorological Society*, 120, 1111–1143.
- Fermepin, S., & Bony, S. (2014). Influence of low-cloud radiative effects on tropical circulation and precipitation. *Journal of Advances in Modeling Earth Systems*, 6, 513–526. <https://doi.org/10.1002/2013MS000288>
- Fuchs, Z., & Raymond, D. (2002). Large-scale modes of a non-rotating atmosphere with water vapor and cloud-radiation feedbacks. *Journal of the Atmospheric Sciences*, 59, 1669–1679.
- Guo, Z., Zhou, T., Wang, M., & Qian, Y. (2015). Impact of cloud radiative heating on East Asian summer monsoon circulation. *Environmental Research Letters*, 10, 074014.
- Held, I., & Hou, A. (1980). Nonlinear axially symmetric circulations in a nearly inviscid atmosphere. *Journal of the Atmospheric Sciences*, 37, 515–533.
- Huffman, G., Adler, R. F., Bolvin, D. T., Gu, G., Nelkin, E. J., Bowman, K. P., et al. (2007). The TRMM multisatellite precipitation analysis (TMPA): Quasi-global multiyear, combined sensor precipitation estimates at fine scales. *Journal of Hydrometeorology*, 8, 38–55.
- Hurley, J., & Boos, W. (2013). Interannual variability of monsoon precipitation and local subcloud equivalent potential temperature. *Journal of Climate*, 26, 9507–9527.
- Inoue, K., & Back, L. (2015). Column-integrated moist static energy analysis on various time scales during TOGA COARE. *Journal of the Atmospheric Sciences*, 72, 1856–1871.
- Inoue, K., & Back, L. (2017). Gross moist stability analysis: Assessment of satellite-based products in the GMS plane. *Journal of the Atmospheric Sciences*, 74, 1819–1837.
- Kuang, Z., Blossey, P., & Bretherton, C. (2005). A new approach for 3D cloud-resolving simulations of large-scale atmospheric circulation. *Geophysical Research Letters*, 32, L02809. <https://doi.org/10.1029/2004GL021024>
- Lee, J.-Y., Wang, B., Wheeler, M., Fu, X., Waliser, D., & Kang, I.-S. (2013). Real-time multivariate indices for the boreal summer intraseasonal oscillation over the Asian summer monsoon region. *Climate Dynamics*, 40, 493–509.
- Lindzen, R., & Hou, A. (1988). Hadley circulations for zonally averaged heating centered off the equator. *Journal of the Atmospheric Sciences*, 45, 2416–2427.
- Luo, Z., & Stephens, G. (2006). An enhanced convection-wind-evaporation feedback in a superparameterization GCM (SP-GCM) depiction of the Asian summer monsoon. *Geophysical Research Letters*, 33, L06707. <https://doi.org/10.1029/2005GL025060>
- Ma, D., Boos, W., & Kuang, Z. (2014). Effects of orography and surface heat fluxes on the South Asian summer monsoon. *Journal of Climate*, 27, 6647–6659.
- Maloney, E. D. (2009). The moist static energy budget of a composite tropical intraseasonal oscillation in a climate model. *Journal of Climate*, 22(3), 711–729.
- National Centers for Environmental Prediction/National Weather Service/NOAA/U.S. Department of Commerce (2000). NCEP FNL Operational Model Global Tropospheric Analyses, continuing from July 1999. Research Data Archive at the National Center for Atmospheric Research, Computational and Information Systems Laboratory. <https://doi.org/10.5065/D6M043C6>
- Nie, J., Boos, W., & Kuang, Z. (2010). Observational evaluation of a convective quasi-equilibrium view of monsoons. *Journal of Climate*, 23, 4416–4428.
- Pauluis, O., & Held, I. M. (2002a). Entropy budget of an atmosphere in radiative-convective equilibrium. Part I: Maximum work and frictional dissipation. *Journal of the Atmospheric Sciences*, 59, 125–139.
- Pauluis, O., & Held, I. M. (2002b). Entropy budget of an atmosphere in radiative-convective equilibrium. Part II: Latent heat transport and moist processes. *Journal of the Atmospheric Sciences*, 59, 140–149.
- Plumb, R. A., & Hou, A. (1992). The response of a zonally symmetric atmosphere to subtropical thermal forcing threshold behavior. *Journal of the Atmospheric Sciences*, 49, 1790–1799.
- Prive, N., & Plumb, R. A. (2007). Monsoon dynamics with interactive forcing. Part II: Impact of eddies and asymmetric geometries. *Journal of the Atmospheric Sciences*, 64, 1431–1442.
- Radel, G., Mauritsen, T., Stevens, B., Dommenget, D., Matei, D., Bellomo, K., & Clement, A. (2009). Amplification of El Niño by cloud longwave coupling to atmospheric circulation. *Nature Geoscience*, 9, 106–110.
- Raymond, D., Sessions, S., Sobel, A., & Fuchs, Z. (2009). The mechanics of gross moist stability. *Journal of Advances in Modeling Earth Systems*, 1, 9. <https://doi.org/10.3894/JAMES.2009.1.9>
- Schneider, T., Bischoff, T., & Haug, G. (2014). Migrations and dynamics of the intertropical convergence zone. *Nature*, 513(7516), 45–53.
- Schneider, T., & Bordoni, S. (2008). Eddy-mediated regime transitions in the seasonal cycle of a Hadley circulation and implications for monsoon dynamics. *Journal of the Atmospheric Sciences*, 65(3), 915–934.
- Shaw, T. (2014). On the role of planetary-scale waves in the abrupt seasonal transition of the Northern Hemisphere general circulation. *Journal of the Atmospheric Sciences*, 71(5), 1724–1746.
- Singh, M. S., Kuang, Z., & Tian, Y. (2017). Eddy influences on the strength of the Hadley circulation: Dynamic and thermodynamic perspectives. *Journal of the Atmospheric Sciences*, 74, 467–486.
- Singh, M. S., & O’Gorman, P. A. (2016). Scaling of the entropy budget with surface temperature in radiative-convective equilibrium. *Journal of Advances in Modeling Earth Systems*, 8, 1132–1150. <https://doi.org/10.1002/2016MS000673>
- Sobel, A. H., & Maloney, E. (2012). An idealized semi-empirical framework for modeling the Madden-Julian Oscillation. *Journal of the Atmospheric Sciences*, 69(5), 1691–1705.
- Sobel, A., Wang, S., & Kim, D. (2014). Moist static energy budget of the MJO during DYNAMO. *Journal of the Atmospheric Sciences*, 71, 4276–4291.
- Sperber, K., Annamalai, H., Kang, I.-S., Kitoh, A., Moise, A., Turner, A., et al. (2014). The Asian summer monsoon: An intercomparison of CMIP5 vs. CMIP3 simulations of the late 20th century. *Climate Dynamics*, 41, 2711–2744.
- Stevens, B., Bony, M., & Webb, M. (2012). Clouds On-Off Climate Intercomparison Experiment (COOKIE). Retrieved from <http://www.euclipse.eu/wp4/wp4.html>

- Voigt, A., & Shaw, T. (2015). Circulation response to warming shaped by radiative changes of clouds and water vapour. *Nature Geoscience*, *8*, 102–106.
- Wang, B., Kang, I.-S., & Lee, J.-Y. (2004). Ensemble simulations of Asian-Australian monsoon variability by 11 AGCMs. *Journal of Climate*, *17*, 803–818.
- Webster, P. (2004). Mechanisms of monsoon low-frequency variability: Surface hydrological effects. *Journal of the Atmospheric Sciences*, *40*, 2110–2124.
- Webster, P., Magana, V., Palmer, T., Shukla, J., Tomas, R., Yanai, M., & Yasunari, T. (1998). Monsoons processes, predicatability, and the prospects for prediction. *Journal of Geophysical Research*, *103*, 14,451–14,510. <https://doi.org/10.1029/97JC02719>
- Xie, S.-P., & Saiki, N. (1999). Abrupt onset and slow seasonal evolution of summer monsoon in an idealized GCM simulation. *Journal of the Meteorological Society of Japan*, *77*, 949–968.